Int. J. Nav. Archit. Ocean Eng. (2015) 7:157~173
http://dx.doi.org/10.1515/ijnaoe-2015-0012
pISSN: 2092-6782, eISSN: 2092-6790

Welding deformation analysis based on improved equivalent strain method considering the effect of temperature gradients

Tae-Jun Kim[1], Beom-Seon Jang[2] and Sung-Wook Kang[2]

[1]*Hyundai Heavy Industries Co., Ltd*
[2]*RIMSE, Department of Naval Architecture and Ocean Engineering, Seoul National University, Seoul, Korea*

ABSTRACT: *In the present study, the existing equivalent stain method is improved to make up for its weaknesses. The improved inherent strain model is built considering more sophisticated three dimensional constraints which are embodied by six cubic elements attached on three sides of a core cubic element. From a few case studies, it is found that the inherent strain is mainly affected by the changes in restraints induced by changes of temperature-dependent material properties of the restraining elements. On the other hand, the degree of restraints is identified to be little influential to the inherent strain. Thus, the effect of temperature gradients over plate thickness and plate transverse direction normal to welding is reflected in the calculation of the inherent strain chart. The welding deformation can be calculated by an elastic FE analysis using the inherent strain values taken from the inherent strain chart.*

KEY WORDS: Welding deformation; Inherent strain; FE analysis; Equivalent strain method.

INTRODUCTION

In shipyards, ships are constructed by the block building method. Welding inevitably induces distortion of a block, and this accumulates during the sequential fabrication process. As the block erection step accounts for about one-third of the whole shipbuilding process, the accuracy of a block's shape and size has a close relation to the overall efficiency of production in the shipyard. The welding distortions reduce the fabrication accuracy of ship hull blocks, and decrease productivity, due to the amount of correction work that is required. To increase the precision of fabrication, the welding distortion and the exact distortion margin at every fabrication stage should be estimated, to meet the allowable tolerances of ship hull blocks.

The prediction and control of welding distortions at the design stage has been an essential task for shipyards, to ensure higher quality, as well as higher productivity (Jang et al., 2007). The most widely used method is the thermal elasto-plastic analysis method. This method gives a relatively accurate result. However, it is disadvantageous in computational time, because of the non-linearity of material. In order to overcome the above difficulties, some efficient approaches are needed.

Ha (2007) developed a modified equivalent loading method based on the inherent strain that incorporated hardening effects. The proposed method was applied to calculate the residual stress at the HAZ. Jang et al. (2007) developed the welding distortion analysis method for the stiffened curved plate using equivalent load method based on inherent strain method

Corresponding author: *Beom-Seon Jang*, e-mail: *seanjang@snu.ac.kr*

considering the fabrication sequences. Ha and Rajesh (2009) carried out thermal distortion analysis for Thermo-Mechanical Control Process (TMCP) steel using inherent strain.

The main purpose of the present study is to propose an efficient approach to predict the welding deformation, based on inherent strain theory, combined with finite element analysis.

EQUIVALENT STRAIN METHOD BASED ON INHERENT STRAIN

Definition of the inherent strain

The inherent strain is defined mechanically as follows: At first, there is a material object that has no stress distribution. When it is under stress by any causes, stress acting on an element of material is accompanied by strains. Then, the stress is released, by cutting out a small part of material; however, residual and irrecoverable strain may still exist. This strain is regarded as the inherent strain.

It can be explained by means of the three material states shown in Fig. 1 (Lee, 1999). The initial state has no stress distribution (Fig. 1 (a)) inside, and the material experiences a stressed condition, caused by phenomena such as thermal strain (Fig. 1 (b)); and the stress is partly released, by cutting a part from the material (Fig. 1 (c)).

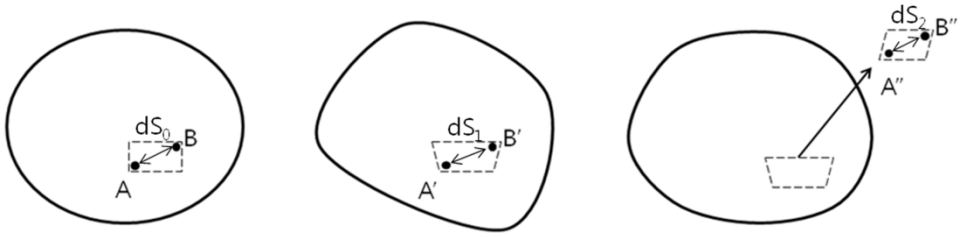

(a) Initial state (stress free). (b) Stressed state. (c) Stress released state.

Fig. 1 Definition of the inherent strain.

Based on the above definition, the inherent strain $\left(\varepsilon^*\right)$ is expressed by subtracting the elastic strain from the total strain,

$$\varepsilon^* = \frac{dS_2 - dS_0}{dS_0} \tag{1}$$

The total strain can be divided into the thermal, plastic, and elastic strains,

$$\varepsilon = \varepsilon^{th} + \varepsilon^{p} + \varepsilon^{e} \tag{2}$$

The inherent strain is defined as the sum of irrecoverable strains, or difference between total strain and elastic strain. (Ha, 2007).

$$\varepsilon^* = \varepsilon^{th} + \varepsilon^{p} = \varepsilon - \varepsilon^{e} \tag{3}$$

Welding analysis based on inherent strain

The distortion and residual stress are computed by elastic analysis, imposing the inherent strain as the initial strain, in the inherent strain method. Inherent strains always remains along the weld bead, and in the nearby zone. It is considered as a source of welding deformation.

The inherent strain is used to two different methods: the equivalent loading method and the equivalent strain method. As for its application, the equivalent strain method (= strain boundary method) is common, and it contains the equivalent loading

method by integrating strain. The equivalent loading method is used to predict welding deformation, by imposing equivalent concentrated loads (Lee, 2002), which are converted from the inherent stress remaining along the heat affected zone (Jang et al., 1997). Its demerit is that it is incapable of predicting welding residual stress.

In the equivalent strain method, the equivalent strain is directly applied to the model. By omitting the process of calculating the equivalent loads, the analysis time is shortened, while the results become more accurate. Its strength is that it enables the evaluation of welding residual stresses, as well as the welding deformation. The procedure is explained in Fig. 2.

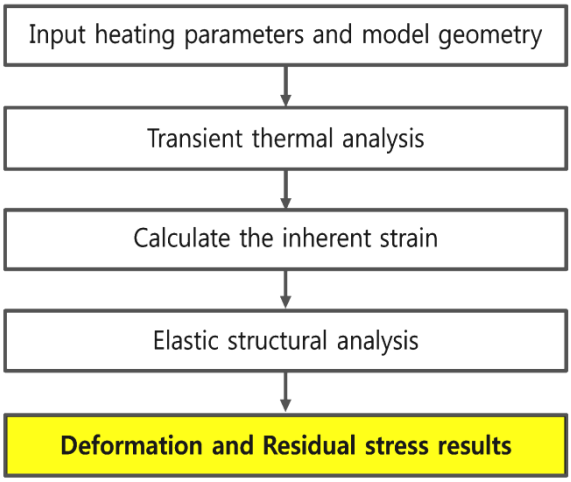

Fig. 2 Procedure for prediction of the deformation and residual stress, using the equivalent strain method.

Calculation of the inherent strain in a previous equivalent strain method

Two important factors to determine the equivalent strain are the highest temperature, and the degree of restraint (Murakawa et al., 1996). The highest temperature indicates the maximum temperature that each point reaches in the heat affected zone, through the whole welding time. The degree of restraint represents the level of resistance against thermal deformation. After calculation of the highest temperature and the degree of restraint, the inherent strains are determined, through an integration process in the inherent strain region. The value of the inherent strain differs, depending on the way of idealizing the heat affected zone.

In a recent study, the inherent strain distribution can be formulated using a simplified thermal elasto-plastic analysis model, as shown in Fig. 3 (Kim, 2010). The heat affected zone is idealized as the solid element (termed 'core'), and adjacent regions putting a restraint on the core are idealized as spring elements (termed 'periphery'). The restraint degree in the thickness direction is omitted, since it is assumed to not be significantly effective in the deformation.

The analysis results are shown in Fig. 4. The $x-axis$ is the degree of restraint in the range from 0.01 to 0.99, and the $y-axis$ is the inherent strain. Each graph is organized according to the highest temperature, in the range from 200 to 1500 °C.

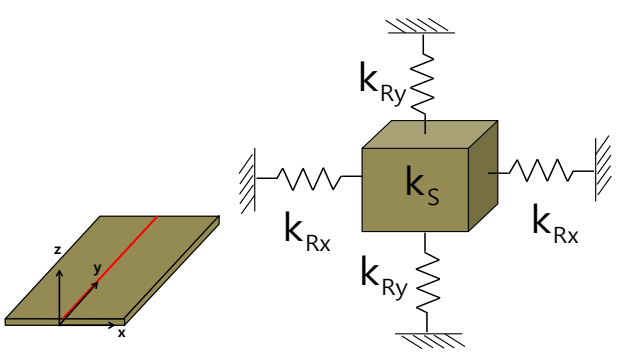

Fig. 3 Simplified thermal elasto-plastic analysis model.

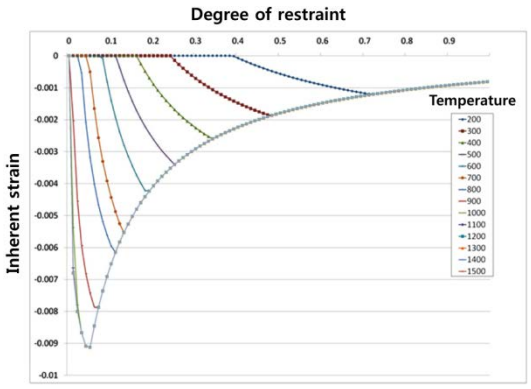

Fig. 4 Inherent strain chart of butt-welding.

Heat transfer analysis is conducted to calculate the temperature distribution of welded structures. The welding heat source is modeled as a normal-distributed moving heat flux. The highest temperature at each node in the finite element model is calculated by the heat transfer analysis.

The degree of restraint of a stiffened panel is determined from the analogy of the solid-spring model, and the elastic FE analysis, using unit load. This method applies unit loads to points where the inherent strains are inputted. Fig. 5 shows the procedure to calculate equivalent strain.

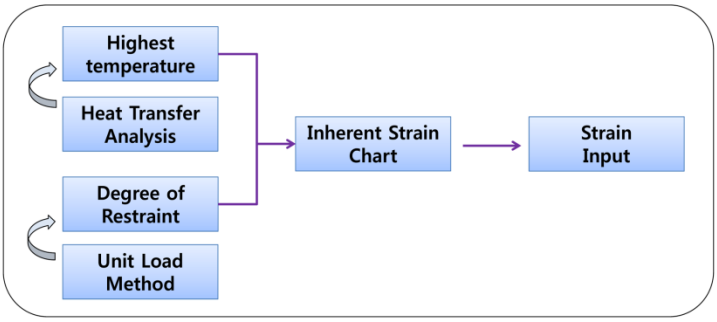

Fig. 5 Calculation of equivalent strain.

LIMITATION OF THE EQUIVALENT STRAIN METHOD IN PREVIOUS STUDY

The temperature of the core element increases to the highest temperature $(T_{\max})$, and then returns to room temperature (T_0). If $T_{\max}$ reaches sufficiently high temperature, the heating and cooling process of the elasto-perfectly plastic model can be divided into four stages, as shown in Fig. 6.

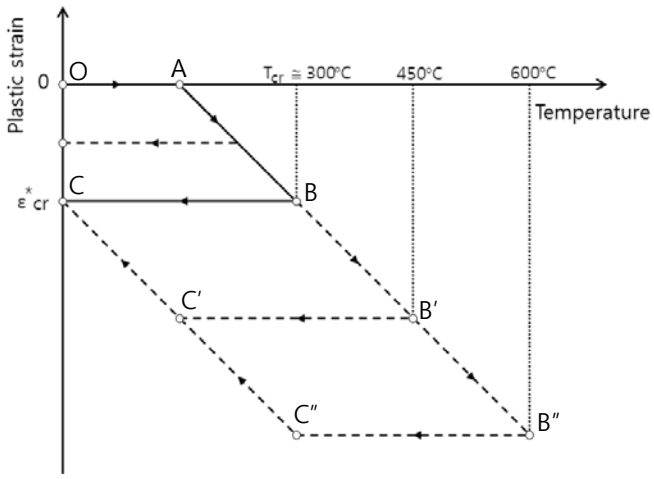

Fig. 6 Thermal history of plastic strain.

While the temperature rises to 450 °*C*, then drops to room temperature, the plastic strain varies along the path $O \to A \to B' \to C' \to C$. OA is an elastic interval. The compressive elastic strain increases, and the plastic strain begins at A. The compressive plastic strain grows constantly in AB'. As cooling starts, elastic strain occurs again in $B'C'$, which is twice the length of OA. In this stage, the compressive elastic strain changes into tensile strain, and elastic tensile strain arrives at the limit, point C'. Then, the compressive plastic strain decreases along the same slope as that of AB', and eventually reaches the point C.

Since the slope of the plastic deformation section, and the length of the elastic deformation section are the same, the residual plastic strain is also the same, as long as the highest temperature is over 300 °*C*. Considering material non-linearity, the shape of

the graph is altered without any fundamental change, even if it does not correspond to the experimental results, or thermal elasto-plastic analysis results.

Fig. 7 shows the highest temperature and residual plastic strain distributions of the same FE model, with different heat input (Case I, II and III). In each case, the plastic strain distribution is different, depending on the highest temperature. Furthermore, the plastic strain value differs according to the distribution of the surrounding temperature, even if the degree of restraint and the highest temperature are exactly the same, as depicted in Case IV and V.

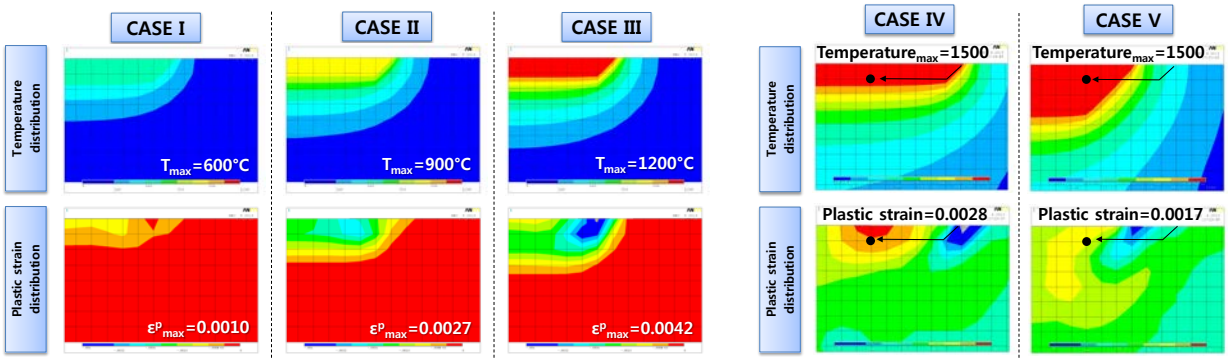

Fig. 7 Temperature and residual plastic strain distributions of same FE model with different heat input.

This is because the inherent strain model improperly uses the assumption of the equivalent loading method. The welding model is completely divided into two regions of heat affected zone, and the periphery, in the equivalent loading method. At this time, it is assumed that the temperature gradient of the periphery is neglected.

In the equivalent inherent strain method, equivalent strains are directly inputted, instead of equivalent loads. Therefore, continuity of the actual temperature distribution should be considered. The temperature and inherent strain are continuously distributed from the region of heat input, to the region free from the heat input. In order to find the inherent strain of elements, even temperature dependent characteristics of the periphery should be taken into account.

IMPROVED EQUIVALENT STRAIN METHOD CONSIDERING THE TEMPERATURE DISTRIBUTION

Improved solid-spring model

When a small part of a material expands or shrinks by the temperature gradient due to welding, the restraint force acts largely on the horizontal plane, rather than the vertical plane of the force direction, as shown in Fig. 8.

As shown in Fig. 9, under the condition that the load in the same direction is applied, and Poisson's ratio of the model is zero, an element on the left is subject to resistance from the normal surface shared by two vertically adjacent elements. However, an element on the right is free from the resistance of the periphery subject to this load. This means that the resistance to the force that drives to expand or shrink in the lateral direction would increase, when the rigidity of two vertically attached elements becomes greater.

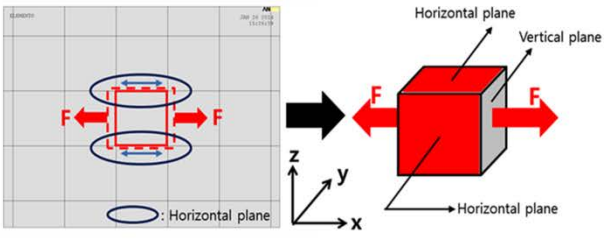

Fig. 8 Working surface of the restraint.

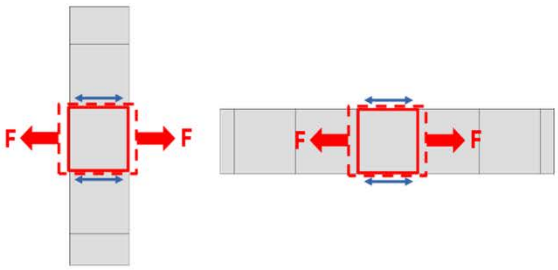

Fig. 9 Extreme cases of the working surface of restraint.

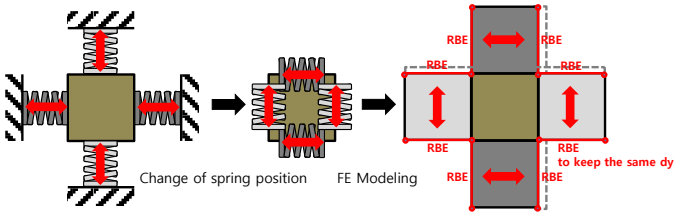

Fig. 10 Biaxial restraints model.

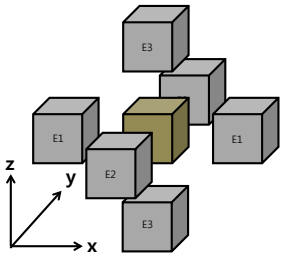

Fig. 11 Disassembled view of the tri-axial restraints model.

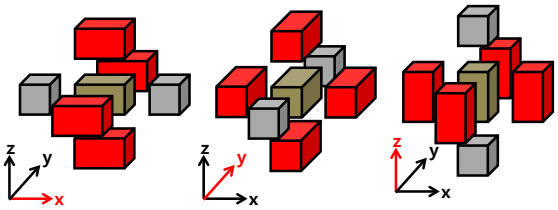

Fig. 12 Restraining elements for each load direction.

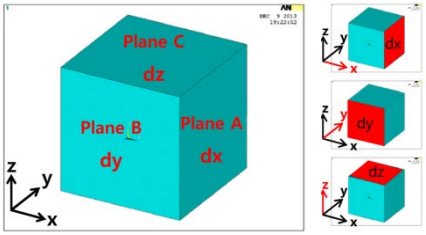

Fig. 13 Boundary condition on the core element.

The proposed restraint model is closer to the actual phenomenon, and more intuitive, by placing proper elements matching the actual restraint. The process of modifying the restraining position of the existing model, and generating an FE model, is shown in Figs. 10-12. All elements, except Rigid Body Elements (RBEs), are in the form of a regular hexahedron. The modification is extended into three dimensions.

A solid-spring model is considered to be axially symmetric. One of the two faces normal to each axis is fixed, and the other is allowed to move freely along the axis. This boundary condition prevents a rigid body motion, without disturbing the intended structural behavior. The boundary condition adopted in this analysis is depicted in Fig. 13.

The elastic modulus of the periphery to induce the equivalent restraint is determined through the following process.

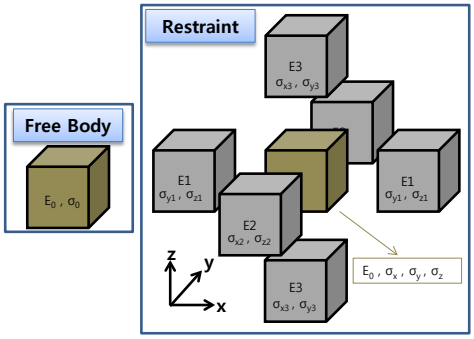

Fig. 14 Definition of stress.

The left box of Fig. 14 contains a core element without restraint, and the right box of Fig. 14 is a core element that is subject to restraints by the neighboring elements. If each system is under the same tri-axially identical unit stress σ_0, the degree of restraint can be expressed by the ratio of strain (ε') of a core element subject to restraint by the periphery, to that (ε_0) without restraint. The degree of restraint is defined as follows.

$$\text{Degree of restraint} \quad k = \frac{\varepsilon_0 - \varepsilon'}{\varepsilon_0} \tag{4}$$

Based on the definition of the restraint model, as represented in Fig. 12, the unit stress σ_0 applied to the model is divided into the unknown stress, such as $\sigma_{x2}, \sigma_{x3}, \sigma_{y3}, ..., \sigma_{z2}$. Thus, the equation of equilibrium is

$$\begin{aligned}\sigma_0 &= \sigma_x + 2(\sigma_{x2} + \sigma_{x3}) \\ &= \sigma_y + 2(\sigma_{y3} + \sigma_{y1}) \\ &= \sigma_z + 2(\sigma_{z1} + \sigma_{z2})\end{aligned} \tag{5}$$

$\sigma_0 =$ unit stress
$\sigma_x, \sigma_x, \sigma_y =$ stress of a core element
$\sigma_{x2}, \sigma_{x3}, \sigma_{y3}, ..., \sigma_{z2} =$ stress of periphery elements

Definitions of the above-defined stresses are illustrated in Fig. 14. The indices 1, 2 and 3 in the subscript indicate the positions of restraining elements that are attached perpendicular to the $x, y,$ and $z-axes$, respectively. The characters, $x, y,$ and z represent the direction of stress of each element.

An element of material subjected to normal stresses $\sigma_x, \sigma_y,$ and σ_z acting in three mutually perpendicular directions is said to be in a state of tri-axial stress. If the material follows Hooke's law, the relationship between the normal stresses and normal strains can be obtained. Strains induced by the stresses $\sigma_x, \sigma_y,$ and σ_z that are acting independently are superimposed, to obtain the resultant strains. Thus, the following equations are derived in tri-axial stress:

$$\begin{aligned}\varepsilon_x &= \frac{1}{E}\left[\sigma_x - \nu(\sigma_y + \sigma_z)\right] \\ \varepsilon_y &= \frac{1}{E}\left[\sigma_y - \nu(\sigma_z + \sigma_x)\right] \\ \varepsilon_z &= \frac{1}{E}\left[\sigma_z - \nu(\sigma_x + \sigma_y)\right]\end{aligned} \tag{6}$$

In this model, by definition of the degree of restraint,

$$\begin{aligned}\frac{1}{E_0}\left[\sigma_x - \nu(\sigma_y + \sigma_z)\right] &= \frac{1}{E_0}(1-k_x)(1-2\nu)\sigma_0 \\ \frac{1}{E_0}\left[\sigma_y - \nu(\sigma_z + \sigma_x)\right] &= \frac{1}{E_0}(1-k_y)(1-2\nu)\sigma_0 \\ \frac{1}{E_0}\left[\sigma_z - \nu(\sigma_x + \sigma_y)\right] &= \frac{1}{E_0}(1-k_z)(1-2\nu)\sigma_0\end{aligned} \tag{7}$$

Since the strain of the core element is the same as those of periphery elements, as explained by the definition of the restraint model, the following equations are derived:

$$\begin{aligned}\varepsilon_x' &= \frac{1}{E_0}[\sigma_x - \nu(\sigma_y + \sigma_z)] = \frac{1}{E_2}[\sigma_{x2} - \nu\sigma_{z2}] = \frac{1}{E_3}[\sigma_{x3} - \nu\sigma_{y3}] \\ \varepsilon_y' &= \frac{1}{E_0}\left[\sigma_y - \nu(\sigma_z + \sigma_x)\right] = \frac{1}{E_3}(\sigma_{y3} - \nu\sigma_{x3}) = \frac{1}{E_1}(\sigma_{y1} - \nu\sigma_{z1}) \\ \varepsilon_z' &= \frac{1}{E_0}\left[\sigma_z - \nu(\sigma_x + \sigma_y)\right] = \frac{1}{E_1}(\sigma_{z1} - \nu\sigma_{y1}) = \frac{1}{E_2}(\sigma_{z2} - \nu\sigma_{x2})\end{aligned} \tag{8}$$

Clearing the variables $\sigma_x, \sigma_x, \sigma_y$ and $\sigma_{x2}, \sigma_{x3}, \sigma_{y3}, ..., \sigma_{z2}$, by simultaneously solving the Eqs. of (7) and (8), the elastic moduli of the periphery to induce the equivalent restraint are defined as follows.

$$
\begin{aligned}
E_1 &= f_1\left(k_x, k_y, k_z\right) = \frac{\frac{Y+vZ}{Z+vY} - v}{Y} \times \frac{\frac{X+vZ}{Z+vX} C + \frac{X+vY}{Y+vX} B - A}{\frac{X+vZ}{Z+vX} + \frac{X+vY}{Y+vX}\frac{Y+vZ}{Z+vY}} \times E_0 \\
E_2 &= f_2\left(k_x, k_y, k_z\right) = \frac{\frac{Z+vX}{X+vZ} - v}{Z} \times \frac{\frac{Y+vX}{X+vY} A + \frac{Y+vZ}{Z+vY} C - B}{\frac{Y+vX}{X+vY} + \frac{Y+vX}{X+vY}\frac{Z+vX}{X+vZ}} \times E_0 \\
E_3 &= f_3\left(k_x, k_y, k_z\right) = \frac{\frac{X+vY}{Y+vX} - v}{X} \times \frac{\frac{Z+vY}{Y+vZ} B + \frac{Z+vX}{X+vZ} A - C}{\frac{Z+vY}{Y+vZ} + \frac{Z+vX}{X+vZ}\frac{X+vY}{Y+vX}} \times E_0
\end{aligned}
\tag{9}
$$

where,

$$
A = \frac{1}{2}\frac{(1-v)k_x + v\left(k_y + k_z\right)}{1+v}, \quad X = \frac{1}{E_0}(1-k_x)(1-2v)
$$

$$
B = \frac{1}{2}\frac{(1-v)k_y + v\left(k_z + k_x\right)}{1+v}, \quad Y = \frac{1}{E_0}(1-k_y)(1-2v)
$$

$$
C = \frac{1}{2}\frac{(1-v)k_z + v\left(k_x + k_y\right)}{1+v}, \quad Z = \frac{1}{E_0}(1-k_z)(1-2v)
$$

Degree of restraint determination

The degree of restraint of the welding model is also expressed in the same manner as the inherent model: by the ratio of a core element strain under restraint (ε' , Fig. 15b) by periphery, to that without restraint (ε_0 , Fig. 15a).

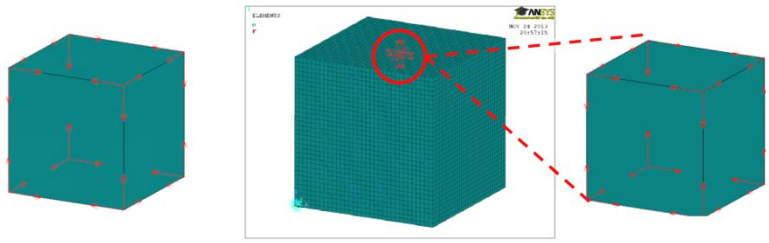

(a) (b)

Fig. 15 Unit load method of the welding model.

The noticeable point is that plastic strain does not occur, if the element has an isotropic degree of restraint in all directions. When plastic yielding occurs, Poisson's ratio is 0.5. Therefore, the plastic strain is always zero, as follows.

$$
\varepsilon^p = \frac{1}{E}\left[\left(1-2\times 0.5\right)\sigma\right] = 0 \tag{10}
$$

If the axial degrees of restraints are different from each other, this causes different axial stresses, and plastic strain can occur during the thermal process.

The resultant absolute plastic strains in the x and y directions become larger, as the difference in the degree of restraints increases, as shown in Table 1. The first two cases are having same k in all direction, the following three cases make the degree of restraint in the z direction different from those of the x and y directions, while maintaining the latter two values the same. The differences are set small in Cases III and IV, while a relatively larger difference obtains in Case V.

Table 1 Relationship between the degree of restraint, and the plastic strain.

CASE	k_x, k_y	k_z	k_x - k_z	ε_x, ε_y	ε_z
I	0.4	0.4	0	0	0
II	0.5	0.5	0	0	0
III	0.45	0.37	0.08	-0.61e-3	1.22e-3
IV	0.55	0.45	0.10	-0.62e-3	1.25e-3
V	0.55	0.15	0.40	-0.85e-3	1.70e-3

The residual plastic strain is found to be dependent on the difference of three axial degrees of restraints. Here, for a plate structure, the actual degrees of restraints are calculated across the thickness, as depicted in Fig. 16. As long as the element size is sufficiently small, all degrees of restraints are the same at any locations, as listed in Table 2. Only the element in the surface has a different value of degree of restraint from the other elements. Even for that element, the difference between the degree of restraint of the in-plane direction and the thickness direction is very small. Also, in a fillet type joint, the difference between the in-plane direction and the thickness direction is zero, or quite small.

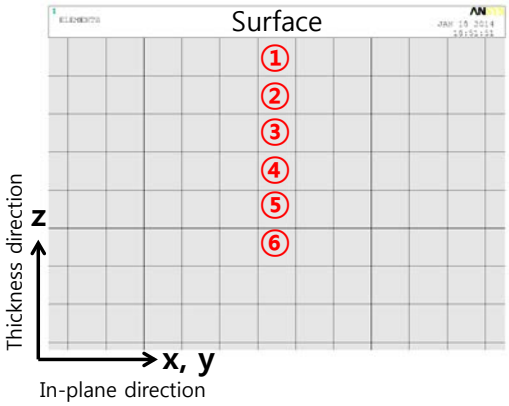

Fig. 16 Degree of restraint calculate location.

Table 2 Degree of restraint.

Location	Degree of restraint		Ratio (In-plane / Thickness)
	In-plane direction, x,y	Thickness direction, z	
①	0.39	0.43	0.91
②	0.56	0.56	1
③	0.57	0.57	1
④	0.57	0.57	1
⑤	0.57	0.57	1
⋮	⋮	⋮	⋮

Thus, a value of 0.57 is to be used as the degree of restraint value in all axial directions at room temperature, regardless of the shape of the model and the position for calculation of the inherent strain, using the improved solid-spring model.

Even if there is no significant difference among the three axial degrees of restraints, and plastic strain does not occur when the element has an isotropic degree of restraint, residual plastic strains still remain after the welding process. This is because the degree of restraint varies, due to temperature changes in the welding process, as shown in Fig. 17. That is, different temperature distributions along the three axes can cause a difference in the three axial restraints, and can induce residual plastic strain.

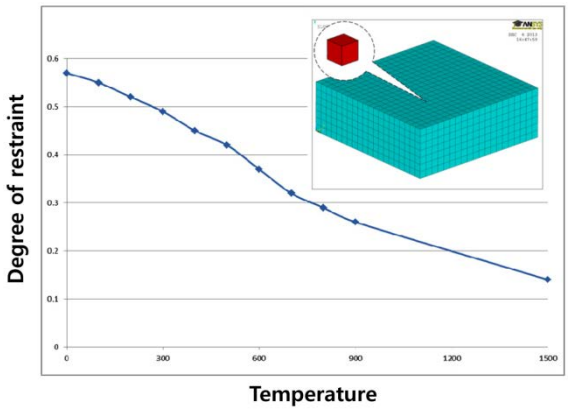

Fig. 17 Temperature-degree of the restraint relation.

Therefore, it is necessary to take into account the changes in the degree of restraints induced by different temperature gradients along the three axial directions. This requires the consideration of the temperature-dependent material property of the peripheral elements, to reflect the continuous changes in the degree of restraints during the welding process.

Inherent strain chart considering temperature gradient

The temperature gradient is represented by an index, termed '*TG*' hereafter. *TG* is a value that is greater than 0, and less than or equal to 1. The temperature gradient is in inverse proportion to the *TG* value.

TG can represent the relative magnitude of the temperature between the core element and the periphery element. For example, when the temperature of a core element is 500 °*C*, and the *TG* value is 1, the temperature of each periphery element is 500 °*C*, as shown in Fig. 18. When the *TG* value is 0.7, the temperature of each periphery element is as shown in Fig. 19. The periphery element of the right hand side has a 30% lower temperature, in comparison with the temperature of the core element; while the periphery element of the left hand side has a 30% higher temperature.

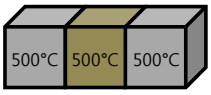

Fig. 18 Temperature gradient at TG=1.

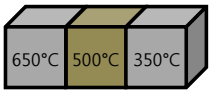

Fig. 19 Temperature gradient at TG=0.7.

Fig. 20 shows the heating and cooling process of the 2D inherent strain model at the highest temperature of 1000 °*C*, while TG_x and TG_y are 0.8 and 0.5, respectively

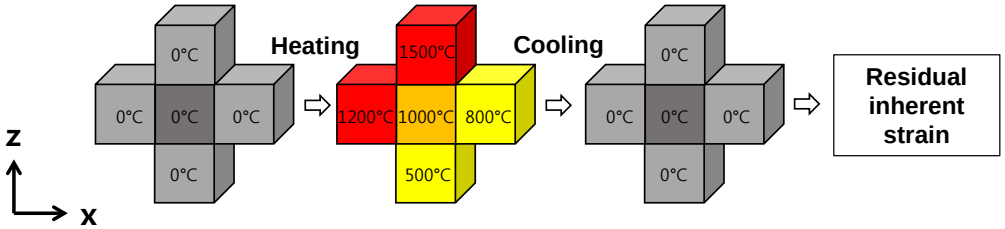

Fig. 20 Temperature gradient at $TG_x = 0.8$, $TG_z = 0.5$.

Fig. 21 explains how to apply TG to an actual welding analysis model. The welding analysis model is divided into two regions, i.e. the 1st and 2nd heat affected zones, depending on the level of temperature variation. Then, TG is determined by the average temperature gradient of each region.

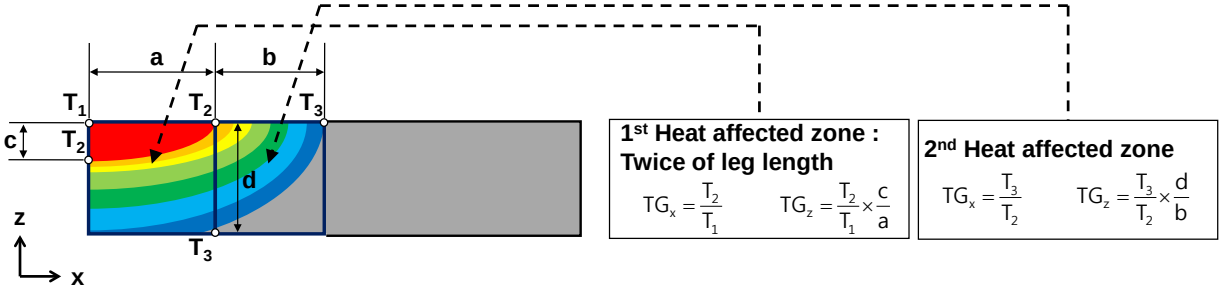

Fig. 21 Definition of TG in the thermal analysis model.

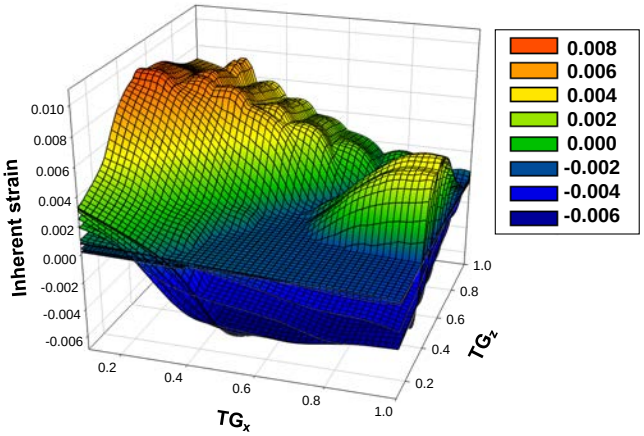

Fig. 22 Inherent strain chart.

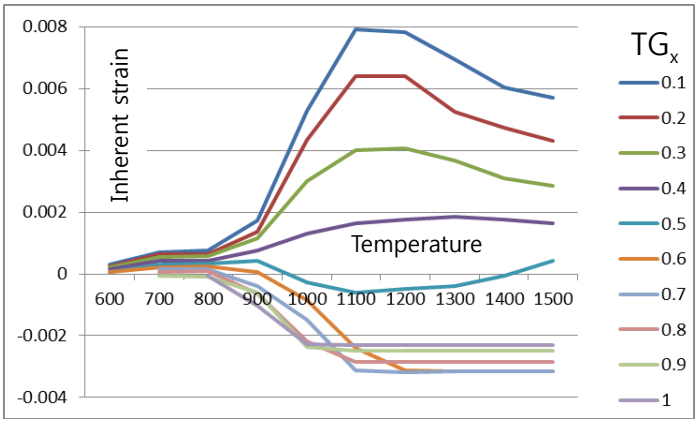

Fig. 23 Inherent strain curve at $TG_z = 0.4$.

The improved inherent strain charts that are obtained by applying the new solid-spring model, and considering the effect of the temperature gradient, are illustrated in Figs. 22-23. The $x, y,$ and $z-axes$ represent $TG_x, TG_z,$ and the inherent strain, respectively. Fig. 22 displays overlapped strain charts for all the highest temperatures. By and large, the absolute value of inherent strain tends to increase, as TG_x gets larger and TG_z smaller, and vice versa. Fig. 23 shows the inherent strain-highest temperature curve at TG_z of 0.4. The inherent strain shifts toward the positive direction, as TG_x becomes smaller; and the negative direction, as TG_z becomes larger.

Welding analysis procedure based on the improved equivalent strain method

Fig. 24 shows the welding analysis procedure, based on the improved equivalent strain method.

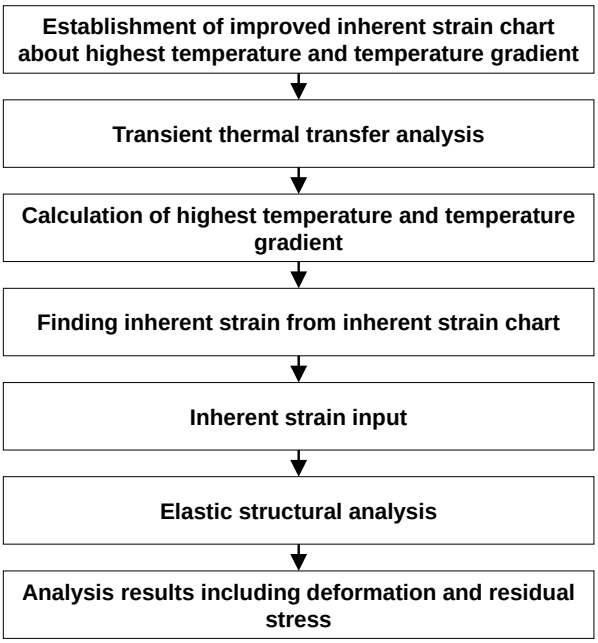

Fig. 24 Welding analysis procedure, using the improved inherent strain method.

WELDING ANALYSIS PROCEDURE USING THE IMPROVED INHERENT STRAIN METHOD

Butt-welding to the experimental data

The analyses of the plate thickness in the range from 6 *mm* to 20 *mm* are performed. The results of thermal Elasto-Plastic Analysis (EPA), existing Equivalent Strain Method (ESM), and Improved Equivalent Strain Method (Improved ESM) are compared with experimental data. The detailed dimensions of the welding models are listed in Table 3. The analysis results are described as follows (Figs. 26-29). Each case is sorted in the order of displacement in the z direction, and residual stress in the x direction. The graphs show the distribution of values in the x direction, which are measured at $y = L/2$ at the top of the plate. The maximum values of angular distortion are listed in Fig. 30.

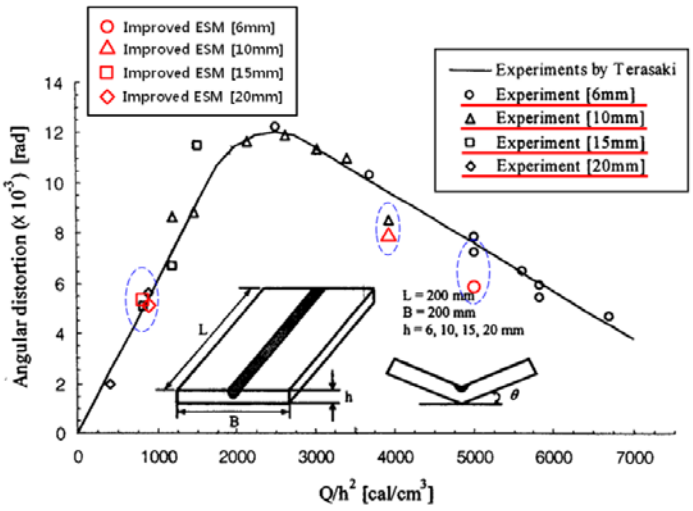

Fig. 25 Comparison with experiment (Sato and Terasaki, 1976).

Table 3 Analysis model dimension and welding condition.

Dimension			Heat
Width [*mm*]	Length [*mm*]	Thickness [*mm*]	Q/h^2 [cal/cm^3]
200	200	6	4880
		10	3830
		15	800
		20	870

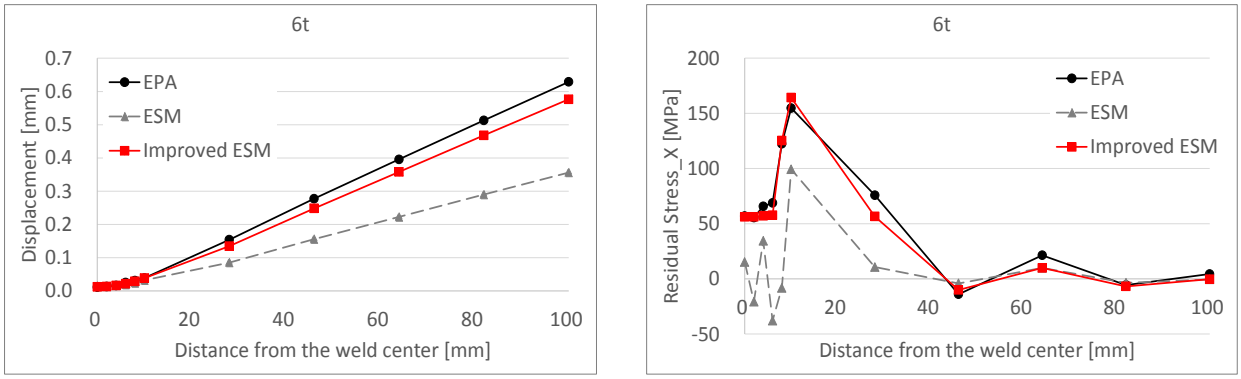

Fig. 26 Displacement (z) and residual stress (x) (t=6 *mm*).

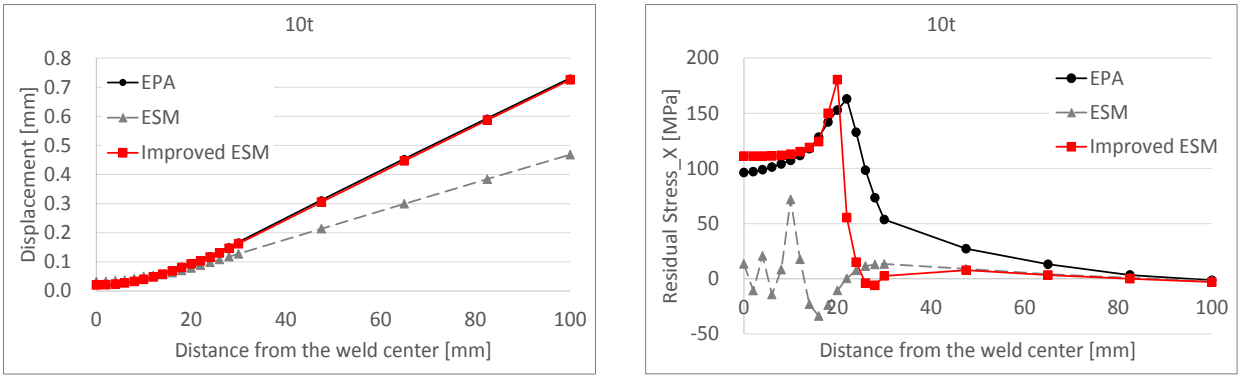

Fig. 27 Displacement (z) and residual stress (x) (t=10 *mm*).

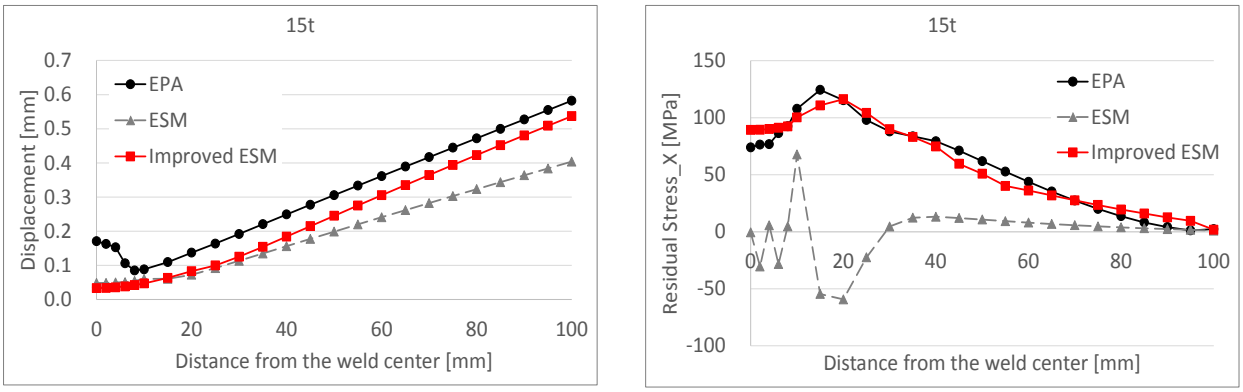

Fig. 28 Displacement (z) and residual stress (x) (t=15 *mm*).

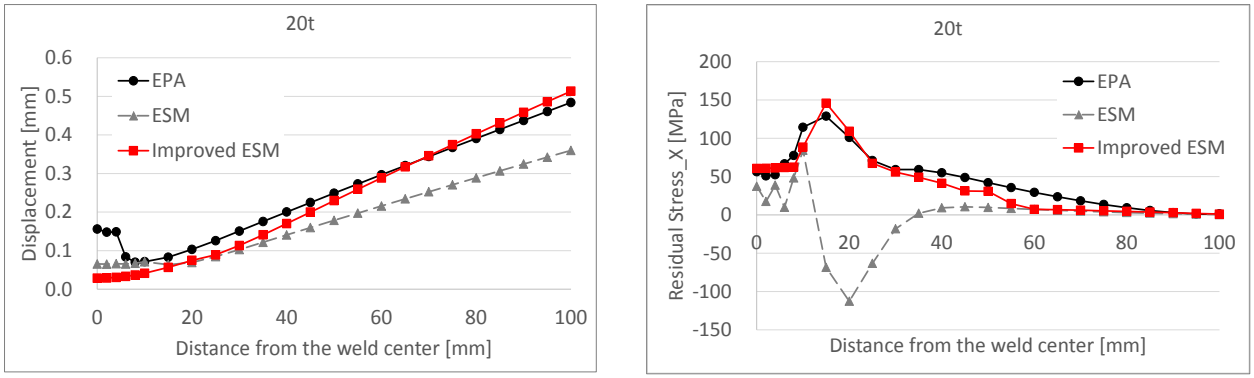

Fig. 29 Displacement (z) and residual stress (x) (t=20 *mm*).

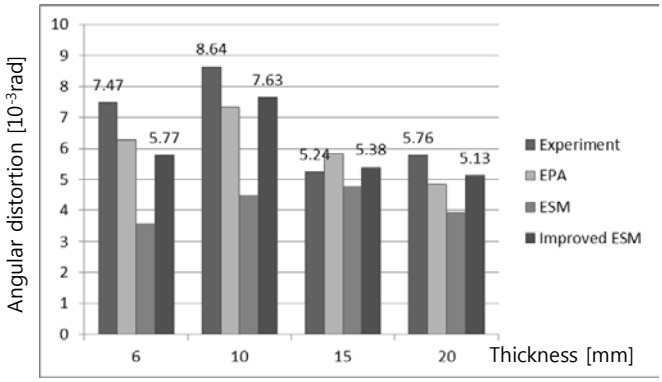

Fig. 30 Angular distortion.

The experimental result and the analysis result based on the Improved ESM, in the case of a 6 *mm* thin plate, show a difference of 23%, slightly larger than for the other cases. However, in the case of a 6 *mm* thin plate, the error between the experiment and the EPA is also the largest. Excluding this, Improved ESM is in good agreement with the experimental results. Only the results of the existing ESM are quite different from those of the other methods, and the experimental data.

Fillet welding

The experimental data of Kim et al. (1996) are used for the fillet welding analysis model. The experimental results are organized by the welding parameter $Q/h^{1.5}$, as shown in Fig. 31. It also indicates analysis results based on the improved equivalent strain method in four models, which refer to the experimental data.

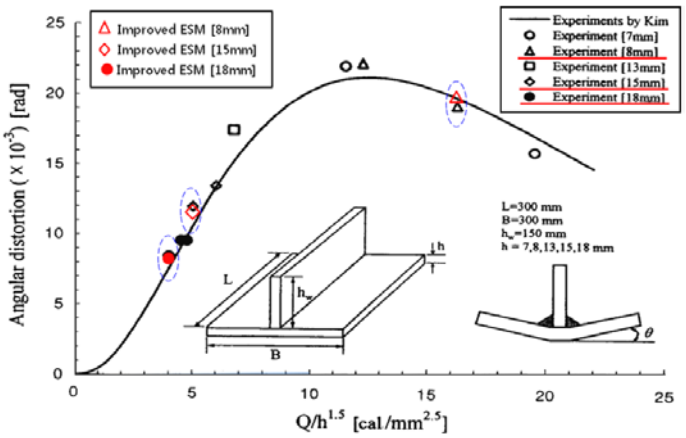

Fig. 31 Comparison with experiment (Kim et al., 1996).

Table 4 Analysis model dimension and welding condition.

Dimension			Heat
Width [*mm*]	Length [*mm*]	Thickness [*mm*]	$Q/h^{1.5}$ [$cal/mm^{2.5}$]
300	300	8	16
		15	5
		18	4

Based on the experimental data, the analysis results of plate thickness in the range from 8 *mm* to 18 *mm* are determined. The results of EPA, ESM and Improved ESM are compared with the experimental data, in the same way as for butt-welding. The welding conditions and detailed dimensions of the welding models are listed in Table 4.

Angular distortions computed by analysis based on the Improved ESM are in good agreement with those of the experimental data, within the error of 5%. The results of the existing ESM are quite different from those of the other methods, and the experimental data. The analysis results are described as follows (Figs. 32-34). The maximum values of angular distortion are listed in Fig. 35.

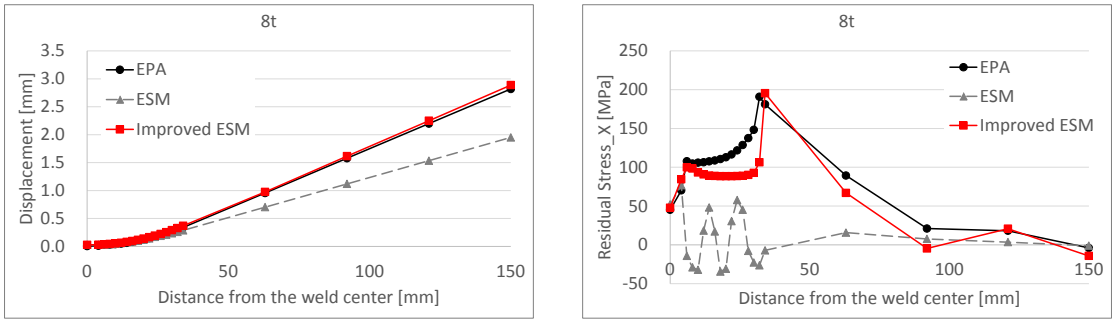

Fig. 32 Displacement (z) and residual stress (x) (t=8 *mm*).

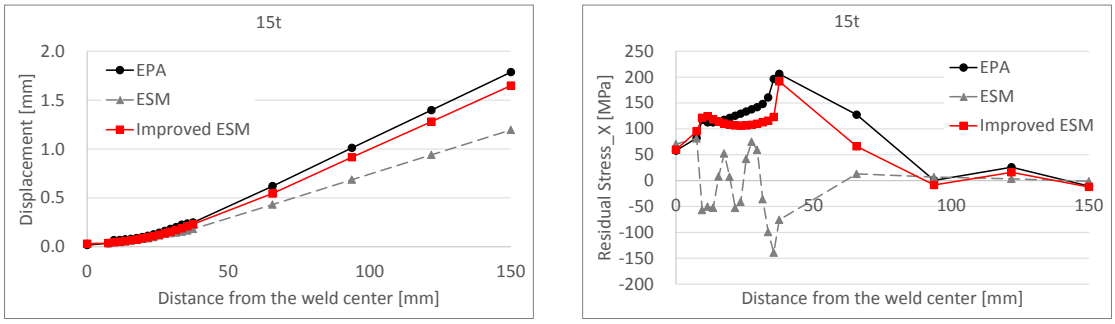

Fig. 33 Displacement (z) and residual stress (x) (t=15 *mm*).

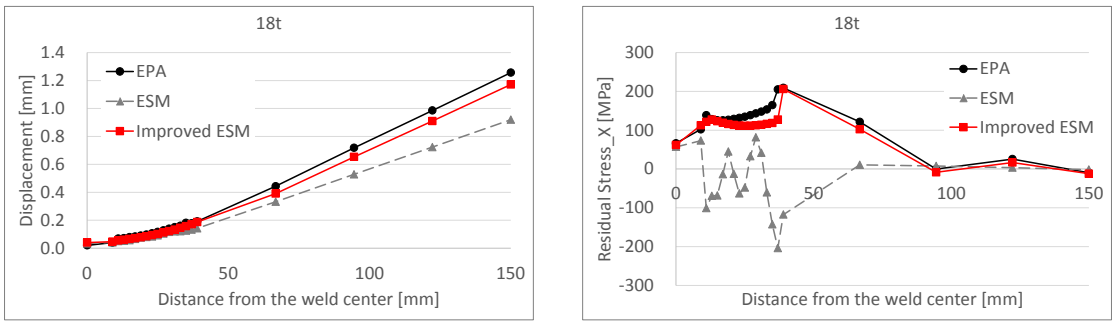

Fig. 34 Displacement (z) and residual stress (x) (t=18 *mm*).

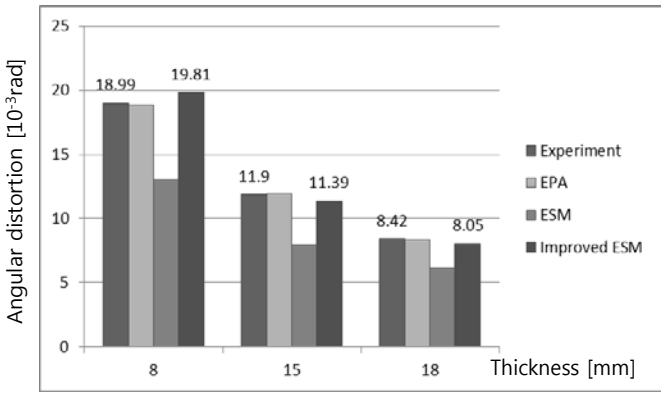

Fig. 35 Angular distortion.

CONCLUSIONS

In the present study, the existing equivalent stain method is improved, to make up for its weaknesses. An improved inherent strain model is built, considering more sophisticated three-dimensional constraints, which are embodied by six cubic elements, attached on three sides of a core cubic element. The effect of temperature gradients over the plate thickness and plate transverse direction normal to the welding is reflected in the calculation of the inherent strain chart.

The proposed method is verified, by comparing the calculated welding deformation analysis results with the existing method, the thermal elasto-plastic FE analysis, and the experimental results.

The main conclusions of the present study are summarized as follows:

1) Two important factors to determine the inherent strain are the highest temperature, and the degree of restraint. However, it is difficult to accurately evaluate the residual deformation and stress of the weld model by these two factors. To make up for these weaknesses, an additional factor that determines the inherent strain is suggested, the temperature gradient.
2) A value of 0.57 is to be used as the degree of restraint value in all axial directions at room temperature for the calculation of inherent strain, regardless of the shape of the analysis model, and the analysis position. Repetitive calculation to find the degree of restraint is no longer required.
3) Improved inherent strain charts that are obtained by applying the new solid-spring model, and considering the effect of the temperature gradient, are suggested. The proposed restraint model is closer to the actual phenomenon, and more intuitive than the previous model, by placing proper elements that match with the actual restraint.
4) The present study develops a quick and accurate method for welding analysis. This result suggests the possibility of analysis for large scaled structure.

ACKNOWLEDGEMENTS

The present work is a result of the project “Development of the design technologies for a 10 *MW* class wave and offshore wind hybrid power generation system and establishment of the sea test infra structure” granted by the Ministry of Oceans and Fisheries, Korea. All support is gratefully acknowledged.

REFERENCES

Ha, Y.S., 2007. Analysis of post-weld deformation at the heat-affected zone using external forces based on the inherent strain. *International Journal of Precision Engineering and Manufacturing*, 8(4), pp.56-62.

Ha, Y.S. and Rajesh, S.R., 2009. Thermal distortion analysis method for TMCP steel structures using shell element. *International Journal of Naval Architecture and Ocean Engineering*, 1(2), pp.95-100.

Jang, C.D., Kim, Y.T., Jo, Y.C. and Ryu, H.S., 2007. Welding distortion analysis of hull blocks using equivalent load method based on inherent strain. *SSC-453*.

Jang, C.D., Seo, S.I. and Ko, D.E., 1997. A Study on the prediction of deformations of plates due to line heating using a simplified thermal elasto-plastic analysis. *Journal of the Society of Naval Architects of Korea*, 34(3), pp.104-112.

Kim, S.I. and Lee, J.S., 1996. Development of Simple Prediction Method for Welding Distortion in Fillet Joints. *Proceedings of the Annual Spring Meeting*, Society of Naval Architecture of Korea, Geoje, Korea, pp.265-270.

Kim, Y.T., 2010. *Structural analysis of ship hull block considering welding residual stress using equivalent strain method based on inherent strain*. Ph. D. Thesis of Seoul National University.

Lee, C.H., 2002. *Prediction of welding deformation of ship full panel blocks using equivalent loading method based on inherent strain*. Ph. D. Thesis of Seoul National University.

Lee, J.H., 1999. *Relations between input parameters and residual deformations in line heating process using finite element method and multi-variate analysis.* Ph. D. Thesis of Seoul National University.

Murakawa, H., Luo, Y. and Ueda, Y., 1996. Prediction of welding deformation and residual stress by elastic FEM based on inherent strain. *Journal of the Society of Naval Architects of Japan*, 180, pp.739-751.

Satoh, K. and Terasaki, T., 1976. Effect of welding conditions on welding deformations in welded structural materials. *Journal of the Japanese Welding Society*, 45(4), pp.54-60.